

Parameter identification in a structured population model

Alexander Lorz* Jan-Frederik Pietschmann† Matthias Schlottbom‡

April 1, 2019

Preprint: April 1, 2019

Abstract

We study parameter identification problems in a structured population model without mutations. Given measurements of the total population size or critical points of the population, we aim to recover its growth rate, death rate or initial distribution. We present uniqueness results under suitable assumptions and present counterexamples when these assumptions are violated. Our results are supplemented by numerical studies, either based on Tikhonov regularization or the use of explicit reconstruction formulas.

1 Introduction

This paper is concerned with the theoretical and numerical study of inverse problems in structured population models. These models describe the coevolution of a population where individuals have a distinct quantitative trait. Examples range from populations of bacteria with different, genetically encoded, abilities to find food sources up to large mammals such as peacocks where the number of eyes on their tail is interpreted as trait or Giraffes with differently sized necks. Denoting by $n = n(t, x)$ the number of individuals with given trait x at time t , a general model for the time evolution of this quantity is

$$\partial_t n(t, x) = s[n(t, x)]n(t, x), \quad x \in \mathbb{R}, t \in (0, T), \quad (1.1)$$

$$n(0, x) = n_0(x). \quad (1.2)$$

The selection rate (or selective pressure) $s[n]$ introduces coupling with respect to the x variable and is assumed to be governed by two effects: Interaction among individuals and interaction with their environment. More precisely, we consider

- *(Asexual) reproduction*: Individuals produce offspring which is of the same trait as its parent (hence asexual reproduction, no mixing of different traits occurs). This is modulated by a reproduction rate $p = p(x)$.

*Sorbonne Université, CNRS, Laboratoire Jacques-Louis Lions, F-75005 Paris, France (on leave). alexander.lorz.uni@gmail.com

†Technische Universität Chemnitz, Fakultät für Mathematik, Reichenhainer Str. 41, 09126 Chemnitz Germany. jfpietschmann@math.tu-chemnitz.de

‡Department of Applied Mathematics, University of Twente, P.O. Box 217, 7500 AE Enschede, The Netherlands. m.schlottbom@utwente.nl

- *Competition*: In many situations, individuals compete for a common but limited resource, e.g., a food source. This is usually modelled by a nonlocal term of the type

$$\int_{\mathbb{R}} K(x, y)n(t, y) dy,$$

where K determines the strength of competition between an individual of type x with one of type y .

- *Mutations*: Even if the reproduction happens asexually, mutation can occur and result in offspring having a different trait than its parent. These mutations are usually “rare” meaning that they happen on a slower timescale than competition and reproduction.

In this work we restrict ourselves to one of the most used choices of $s[n]$ making the assumptions that all individuals compete with the same strength ($K = 1$) and neglecting mutations. This leads to

$$s[n] = p(x) - d(x)\rho(t), \tag{1.3}$$

with reproduction rate p and the trait-dependent weight function d modulating the death rate $d\rho$, and where

$$\rho(t) = \int_{\mathbb{R}} n(t, x) dx \tag{1.4}$$

denotes the total mass of the population at time t . Selection rates of the form (1.3) are frequently used in the literature, see for example [18, 2]. In our case, since $\rho(t)$ is simply the total mass, all individuals are in competition with one another, independent of their particular trait. We note that similar models can also be derived from stochastic models with finite populations, cf. [4, 5, 7].

The dynamics of such equations has been studied extensively by many authors, see, e.g., [6, 11, 16]. Besides existence and uniqueness of solutions, their long time behavior is most relevant for applications. Depending on the particular form of s , it is expected that only a few traits survive for large times, i.e., that the solution converges to a finite sum of Dirac measures. This is strongly related to the notion of evolutionary stable strategy (ESS). According to [17] an ESS corresponds to a situation where “(...) a strategy [exists] such that, if most of the members of a population adopt it, there is no ‘mutant’ strategy that would give higher reproductive fitness”. In our framework, this corresponds to situations where, as $t \rightarrow \infty$, the quantity $n(x, t)$ converges to a single delta distribution. We refer to [6, 14, 15] for more details. In particular, these works formulate conditions on the model parameters that ensure the existence of an ESS.

This leaves us in the following situation: We have a mathematical model for the coevolution of structured populations and analytical results that allow us to predict the long time behaviour of this model which is most important for practical applications. However, to be able to use these criteria in concrete situations and thus to completely close the gap between modelling and applications, detailed knowledge of the model parameters is needed. This motivates our present study of corresponding inverse problems.

Let us also emphasize that, to the best of our knowledge, the present work is the first time that the inverse problem for such a model is analysed and we hope to encourage further research on this type of non-standard state equations.

To begin, let us first discuss possible measurement data. If $n(t, x)$ would be known for all x and t , this would infer knowledge of $\rho(t)$ via (1.4) and of $n_0(x)$. Equation (1.1) with (1.3) then yields the relation

$$\partial_t \ln(n(t, x)) = p(x) - d(x)\rho(t). \quad (1.5)$$

Differentiation with respect to t and assuming that $\rho'(t) \neq 0$, yields a formula for $d(x)$, which then also yields a formula for $p(x)$. Returning, however, to the example of a population of bacteria it becomes clear that one cannot expect to acquire this data in general. Instead, we shall focus on the following two quantities:

Total population size $\rho(t)$: The total population size seems the most natural quantity and is also easy to acquire in many situations. For example in the case of a petri dish containing a population of bacteria, several established methods exist to determine their number, see, e.g., [19]. Even for large animals, extracting the total population number from, e.g., video footage is feasible [3]. This gives rise to the following inverse problem:

(P1) Given measurements of $\rho(t)$ on $[0, T]$, determine either the function $p(x)$, $d(x)$ or $n_0(x)$.

Critical couples: Another possible measurement may be critical points in the population density, i.e., couples $(\bar{t}, \bar{x}) \in [0, T] \times \mathbb{R}$ at which $\partial_x n(\bar{t}, \bar{x}) = 0$ holds. Their biological interpretation is more difficult but consider for example [10], where the authors work with three different bacteria strains. Each one has a temperature depend proliferation rate which can directly be interpreted as trait x . Then, if \bar{x} is the proliferation rate at the optimal temperature, which can be obtained by experiments, one can show that \bar{x} is also a critical point for $n(\bar{t}, \cdot)$. Even if it seems less straight forward to obtain these measurements in other settings, our results can be valuable as a hint for the possible design of future experiments. With these measurements at hand, we consider the following inversion problem:

(P2) Given measurements of critical couples (\bar{t}, \bar{x}) of n , determine either $p(\bar{x})$, $d(\bar{x})$ or $n_0(\bar{x})$.

As will be elaborated below, there exist a number of transformations that can be applied to the parameters p and d that leave the quantities ρ and / or the critical couples of n unchanged. In these situations one cannot expect any positive identification result which is directly reflected in the assumptions we have to make in our uniqueness theorems. More precisely, for (P1), we are able to give a positive identification result under suitable monotonicity assumptions on the parameters and present explicit counterexamples when these assumptions are violated. In situations when uniqueness is guaranteed, we present numerical reconstructions using Tikhonov regularization, and we verify convergence under a standard smoothness assumption. For (P2), we derive explicit formulas for the derivatives p' , d' and n'_0 , which imply uniqueness and stability with respect to perturbations of the measured data. The latter is demonstrated by numerical examples. Finally, we also comment on the simultaneous identification problem:

(P3) Given measurements of $\rho(t)$ as well as the critical couples of n , determine both $p(x)$ and $n_0(x)$.

While a dimensional analysis of data and unknowns suggests a uniqueness result, we cannot give a definite answer. This is mainly due to the fact that it seems very delicate to combine the nonlocal information contained in $\rho(t)$ with the knowledge of critical couples that is purely

local.

This paper is organized as follows: In Section 2, we study the population model and show existence and uniqueness of solutions. In Section 3 we address (P1), give counterexamples to the identification problem for general parameters, and give classes of parameter functions for which the inverse problems in (P1) can be solved uniquely. In Section 4, we consider (P2) and present reconstruction formulas for the derivatives of the parameter functions, which is followed by a discussion regarding (P3). We present extensive numerical results for the actual reconstruction of the unknown parameters, including different ways to treat the (nonlinear) problem as well as convergence rates in Section 5. Finally, in Section 6, we give an outlook for a population model with mutation.

2 Existence of solutions

Equations (1.1)–(1.4) can be understood as a system of ordinary differential equations (for every point $x \in \mathbb{R}$) coupled via $\rho(t)$, which motivates to rewrite the solution using the following implicit representation

$$n(t, x) = n_0(x)e^{tp(x)-d(x)\int_0^t \rho(s) ds}. \quad (2.1)$$

Integrating expression (2.1) with respect to the trait yields the following nonlinear fixed-point equation for the total population

$$\rho(t) = \int_{\mathbb{R}} n_0(x)e^{tp(x)-d(x)\int_0^t \rho(s) ds} dx, \quad (2.2)$$

which is an ordinary differential equation for $R(t) = \int_0^t \rho(s) ds$ with initial data $R(0) = 0$. For convenience of the reader and for later reference, we provide a proof of uniqueness and existence of solutions to (1.1)–(1.4). Let us refer also to [6, Thm 2.1] for a similar strategy, yet in different function spaces.

Theorem 2.1. *Let $p, d \in L^\infty(\mathbb{R})$ and let $n_0 \in L^1(\mathbb{R})$ such that $d \geq 0$ and $n_0 \geq 0$. Then there exists a unique $n \in C^\infty([0, T], L^1(\mathbb{R}))$ and $\rho \in C^\infty([0, T])$ solution to (1.1)–(1.2).*

Proof. The proof relies on Banach's fixed point theorem. For

$$M = \{\rho \in L^\infty(0, T) : \rho \geq 0\}$$

define the map $\Lambda : M \rightarrow M$ as

$$(\Lambda(\rho))(t) = \int_{\mathbb{R}} n_0(x)e^{tp(x)-d(x)\int_0^t \rho(s) ds} dx. \quad (2.3)$$

By construction, fixed points of Λ are solutions to (2.2). We endow the space $L^\infty(0, T)$ with the norm

$$\|\rho\|_{\infty, a} = \sup_{0 < t < T} |\rho(t)|e^{-at}$$

and choose $a = 2\|n_0\|_{L^1}\|d\|_\infty e^{T\|p\|_\infty}$. We have $a = 0$ when either $n_0 \equiv 0$ or $d \equiv 0$, and the assertion holds trivially. Let now $a > 0$. Obviously, Λ is a self-mapping. In order to show that Λ is a contraction, we observe that

$$|e^{-dz} - e^{-dz_0}| \leq d|z - z_0|$$

for all $z_0, z \geq 0$. Hence, we obtain for $\rho_1, \rho_2 \in M$

$$\begin{aligned} |\Lambda(\rho_1) - \Lambda(\rho_2)|(t) &\leq \int_{\mathbb{R}} n_0(x) e^{tp(x)} |e^{-d(x) \int_0^t \rho_1(s) ds} - e^{-d(x) \int_0^t \rho_2(s) ds}| dx \\ &\leq \|n_0\|_{L^1} e^{T\|p\|_\infty} \|d\|_\infty \int_0^t |\rho_1(s) - \rho_2(s)| ds \\ &\leq \|n_0\|_{L^1} e^{T\|p\|_\infty} \|d\|_\infty \|\rho_1 - \rho_2\|_{\infty, a} \frac{e^{at}}{a}. \end{aligned}$$

By the choice of a , we thus obtain

$$\|\Lambda(\rho_1) - \Lambda(\rho_2)\|_{\infty, a} \leq \frac{1}{2} \|\rho_1 - \rho_2\|_{\infty, a},$$

which shows that Λ is a contraction. Banach's fixed point theorem implies the existence and uniqueness of $\rho \in M$ such that $\rho = \Lambda(\rho)$. Defining $n(t, x)$ via (2.1) yields the unique solution to (1.1)–(1.2). In addition, since $t \mapsto \int_0^t \rho(s) ds \in W^{1, \infty}(0, T)$, we infer that $n(t, x) \in W^{1, \infty}(0, T)$ a.e. x . The regularity assumptions on p, d and n_0 yield that $n \in W^{1, \infty}(0, T; L^1(\mathbb{R}))$. Using (1.4), we then obtain $\rho \in W^{1, \infty}(0, T)$. Repeating these arguments, we obtain higher order differentiability in time of ρ and n . \square

Using similar arguments as in the proof of Theorem 2.1, we can show the next result, which is used below in the analysis of Tikhonov regularization for (P1).

Lemma 2.2. Let $d \in L^\infty(\mathbb{R})$ be non-negative and let $n_0 \in L^1(\mathbb{R})$ be non-negative. Moreover, let $C > 0$ be a constant and define the set

$$\mathcal{D}(\Lambda) = \{p \in L^\infty(\mathbb{R}) : 0 \leq p(x) \leq C\} \times \{\rho \in L^2(0, T) : 0 \leq \rho\} \subset L^\infty(\mathbb{R}) \times L^2(\mathbb{R}).$$

Then the map $\Lambda : \mathcal{D}(\Lambda) \rightarrow L^2(0, T)$ defined by $\Lambda_p(\rho) = \int_{\mathbb{R}} n_0(x) e^{tp(x)-d(x) \int_0^t \rho(s) ds} dx$ is Lipschitz continuous.

Proof. Inspecting the proof of Theorem 2.1, we observe that $\rho \mapsto \Lambda_p(\rho)$ for ρ such that $(p, \rho) \in \mathcal{D}(\Lambda)$ satisfies

$$\|\Lambda_p(\rho_1) - \Lambda_p(\rho_2)\|_{L^2(0, T)} \leq \|n_0\|_{L^1} \sqrt{T} e^{CT} \|d\|_\infty \|\rho_1 - \rho_2\|_{L^2(0, T)}.$$

A similar argument shows that $p \mapsto \Lambda_p(\rho)$ for p such that $(p, \rho) \in \mathcal{D}(\Lambda)$ satisfies

$$\|\Lambda_{p_1}(\rho) - \Lambda_{p_2}(\rho)\|_{L^2(0, T)} \leq \|n_0\|_{L^1} \sqrt{T} T e^{CT} \|p_1 - p_2\|_\infty,$$

which concludes the proof. \square

3 Identification from knowledge of the total population size

In the following we address inverse problem (P1). In general, the coefficient p is not uniquely determined given measurements of the total population ρ as shown by the following examples.

- (i) Translational invariance: Let $n_0(x) = 1$ for $x \in \mathbb{R}$, $d = 0$ and let $c > 0$ be arbitrary. In addition, choose a compactly supported function $p(x)$ and define the function $\bar{p}(x) := p(x + c)$. Solving (1.1)–(1.2) with parameters p and \bar{p} , respectively, yields the same function $\rho(t)$.

- (ii) Symmetry: Let $d(x) = d(-x)$, $n_0(x) = n_0(-x)$, and let $p_1(x)$ be arbitrary. If we define $p_2(x) = p_1(-x)$, then $n_2(x, t) = n_1(-x, t)$, and $\rho_1(t) = \rho_2(t)$ for $t \geq 0$.

These examples suggest to consider the class of strictly monotone coefficient functions p .

Theorem 3.1. *Let $n_0 \in C^0(\mathbb{R})$ be nonnegative with compact and connected support. Assume that $d(x) = d > 0$ is constant. Denote by p_1 and p_2 continuous and strictly monotone functions on the support of n_0 such that $p_1' p_2' > 0$, and let n_1 and n_2 denote the solutions to (1.1)–(1.2) with p replaced by p_1 and p_2 , respectively. Then, with ρ_1 and ρ_2 being the respective population sizes we have*

$$\rho_1 = \rho_2 \text{ on } [0, T] \text{ implies } p_1 = p_2 \text{ on } \text{supp}(n_0).$$

Proof. By assumption $\rho = \rho_1 = \rho_2$, and it follows from (1.4) that

$$\int_{\mathbb{R}} n_0 e^{tp_1} e^{-d \int_0^t \rho(s) ds} dx = \int_{\mathbb{R}} n_0 e^{tp_2} e^{-d \int_0^t \rho(s) ds} dx. \quad (3.1)$$

Since d is constant, this implies

$$\int_{\mathbb{R}} n_0 e^{tp_1} dx = \int_{\mathbb{R}} n_0 e^{tp_2} dx.$$

Using monotonicity of p_1 and p_2 , we can transform each of the integrals, using either $y = p_1(x)$ or $y = p_2(x)$ as new variables, respectively, to obtain

$$\int_{\mathbb{R}} \left(\frac{n_0(p_1^{-1}(y))}{p_1'(p_1^{-1}(y))} \chi_{\mathcal{P}_1}(y) - \frac{n_0(p_2^{-1}(y))}{p_2'(p_2^{-1}(y))} \chi_{\mathcal{P}_2}(y) \right) e^{ty} dy = 0,$$

where we also used that $p_1' p_2' > 0$. Here, $\mathcal{P}_i = p_i(\mathcal{S})$ for $\mathcal{S} = \text{supp}(n_0)$, $i = 1, 2$, and $\chi_{\mathcal{P}_i}$ denotes the indicator function of the set \mathcal{P}_i . Since \mathcal{S} is a compact interval and $p_i \in C^0(\mathcal{S})$, \mathcal{P}_i are compact intervals. Differentiation with respect to t and evaluating the result for $t = 0$ then yields, for every $k \geq 0$,

$$\int_{\mathcal{P}_1 \cup \mathcal{P}_2} \left(\frac{n_0(p_1^{-1}(y))}{p_1'(p_1^{-1}(y))} \chi_{\mathcal{P}_1}(y) - \frac{n_0(p_2^{-1}(y))}{p_2'(p_2^{-1}(y))} \chi_{\mathcal{P}_2}(y) \right) y^k dx = 0. \quad (3.2)$$

The term in brackets is continuous as a function of y due to the construction of \mathcal{P}_i , $i = 1, 2$. Since $\mathcal{P}_1 \cup \mathcal{P}_2$ is compact, a density argument yields

$$\frac{n_0(p_1^{-1}(y))}{p_1'(p_1^{-1}(y))} \chi_{\mathcal{P}_1}(y) - \frac{n_0(p_2^{-1}(y))}{p_2'(p_2^{-1}(y))} \chi_{\mathcal{P}_2}(y) = 0 \quad (3.3)$$

for all $y \in \mathcal{P}_1 \cup \mathcal{P}_2$. This readily implies $\mathcal{P}_1 \setminus \mathcal{P}_2 = \emptyset$ and $\mathcal{P}_2 \setminus \mathcal{P}_1 = \emptyset$, and hence $\mathcal{P}_1 \cup \mathcal{P}_2 = \mathcal{P}_1 \cap \mathcal{P}_2$, i.e., $\mathcal{P}_1 = \mathcal{P}_2$. Introducing the primitive of n_0 , i.e.,

$$N_0(x) = \int_{x_0}^x n_0(z) dz,$$

where $x_0 = \min \mathcal{S}$, we see that (3.3) is equivalent to

$$\frac{d}{dy} (N_0(p_1^{-1}(y)) - N_0(p_2^{-1}(y))) = 0$$

for all $y \in \mathcal{P} := \mathcal{P}_1 = \mathcal{P}_2$. The assumption $p'_1 p'_2 > 0$ then implies $p_1(x_0) = p_2(x_0)$, and hence $N_0(p_1^{-1}(y)) = N_0(p_2^{-1}(y))$ for all $y \in \mathcal{P}$. Using the definition of N_0 we thus obtain

$$\int_{p_2^{-1}(y)}^{p_1^{-1}(y)} n_0(z) dz = 0$$

for $y \in \mathcal{P}$. Since, $p_i^{-1}(\mathcal{P}) = \mathcal{S}$, $i = 1, 2$, and n_0 is positive in the interior of \mathcal{S} , we deduce that $p_1^{-1}(y) = p_2^{-1}(y)$ for all $y \in \mathcal{P}$, i.e., $p_1(x) = p_2(x)$ for all $x \in \mathcal{S}$. \square

Remark 3.2 (Identification of d and n_0). *Interchanging the roles of d and p in the above examples shows that, in general, uniqueness of d cannot be expected from knowledge of ρ only. With similar arguments as in the proof of Theorem 3.1, one can, however, prove uniqueness of d in the class of strictly monotone functions (either increasing or decreasing) given measurements of $\rho(t)$ and knowledge of n_0 and constant p . Moreover, one can show that for p and n_0 arbitrary, knowledge of $\rho(t)$, $t \geq 0$, uniquely determines constant parameters d . The transformation $y = p(x)$ in the proof of Theorem 3.1 can also be used to identify compactly supported initial data n_0 if p is strictly monotone and d is constant. We leave the details to the reader.*

4 Identification from critical couples of the population

Above we have shown that, under appropriate assumptions, the total population size contains sufficient information for the determination of some of the parameters of the problem. These results, however, do not provide an explicit reconstruction formula. In this section, we show that knowledge of the critical couples of the population density can be used to directly compute derivatives of the unknown parameters.

Before we state the results, we discuss properties of the critical couples of n in some detail.

4.1 The critical couples of n

We call (\bar{t}, \bar{x}) with $\bar{x} \in \mathbb{R}$ and $\bar{t} \geq 0$ a critical couple of n if $n_0(\bar{x}) > 0$ and $\partial_x n(\bar{t}, \bar{x}) = 0$.

Lemma 4.1. Denote by n the solution to (1.1)–(1.2) for differentiable parameter functions d and p . Then, for any critical couple (\bar{t}, \bar{x}) of n it holds that

$$(\ln(n_0(x)))'_{|x=\bar{x}} = d'(\bar{x}) \int_0^{\bar{t}} \rho(s) ds - \bar{t} p'(\bar{x}). \quad (4.1)$$

Proof. Using the chain rule, we see that (\bar{t}, \bar{x}) is also a critical couple of $\ln n$, i.e.,

$$\partial_x (\ln(n(\bar{t}, x)))_{|x=\bar{x}} = 0.$$

On the other hand, from the solution formula (2.1), we deduce that

$$\ln(n(t, x)) = \ln(n_0(x)) + tp(x) - d(x) \int_0^t \rho(s) ds,$$

so we obtain the result by differentiation with respect to x and evaluation at $x = \bar{x}$ and $t = \bar{t}$. \square

Assuming that d is constant, the critical couples (\bar{t}, \bar{x}) of n satisfy

$$\frac{n'_0(\bar{x})}{n_0(\bar{x})} + \bar{t}p'(\bar{x}) = 0. \quad (4.2)$$

We distinguish three cases:

- (i) For $n'_0(\bar{x})p'(\bar{x}) > 0$, (\bar{t}, \bar{x}) is never a critical couple of n for any $\bar{t} \geq 0$.
- (ii) For $n'_0(\bar{x})p'(\bar{x}) < 0$, there exists a unique $\bar{t} = -n'_0(\bar{x})/(n_0(\bar{x})p'(\bar{x}))$ such that (\bar{t}, \bar{x}) is a critical couple of n .
- (iii) For $n'_0(\bar{x})p'(\bar{x}) = 0$, if $p'(\bar{x}) = 0$, then (4.2) implies $n'_0(\bar{x}) = 0$, and (\bar{t}, \bar{x}) is a critical couple of n for all $\bar{t} \geq 0$. Otherwise, if $p'(\bar{x}) \neq 0$, then (\bar{t}, \bar{x}) is critical couple of n only if $\bar{t} = 0$.

A similar discussion applies for p constant and d variable; or n_0 constant and p and d variable.

4.2 Identification of a single parameter

As a direct consequence of Lemma 4.1 we obtain the following reconstruction formulas for the derivatives of the parameters.

Theorem 4.2. *Let $T > 0$, and denote by n the solution to (1.1)–(1.2) for differentiable functions d and p and differentiable initial datum. Furthermore, let (\bar{t}, \bar{x}) with $\bar{t} > 0$ be a critical couple of n .*

(i) *If d is constant, then $p'(\bar{x})$ is uniquely determined by n_0 , i.e.,*

$$p'(\bar{x}) = -\frac{n'_0(\bar{x})}{\bar{t}n_0(\bar{x})}. \quad (4.3)$$

(ii) *If p is constant, then $d'(\bar{x})$ is uniquely determined by n_0 and $\int_0^{\bar{t}} \rho(s)ds$, i.e.,*

$$d'(\bar{x}) = \frac{n'_0(\bar{x})}{n_0(\bar{x}) \int_0^{\bar{t}} \rho(s)ds}. \quad (4.4)$$

(iii) *$(\ln(n_0(x)))'|_{x=\bar{x}}$ is uniquely determined by $p'(\bar{x})$, $d'(\bar{x})$ and $\int_0^{\bar{t}} \rho(s)ds$ by (4.1).*

Remark 4.3. *It can be easily seen from the solution formula (2.1) that the functions $n(t, x)$ and $n_c(x, t)$, which are solutions to (1.1)–(1.4) for the two parameter functions (p, d) and $(p + c, d)$ with constants $c, d \in \mathbb{R}$, respectively, share the same critical couples. In this sense, the previous theorem cannot be improved without further assumptions. A similar conclusion holds true for parameter pairs (p, d) and $(p, d + c)$.*

Remark 4.4. *In the situation of Theorem 4.2 (i), if the closure of $\{\bar{x} : (\bar{t}, \bar{x}) \text{ is critical for } n\}$ coincides with the support of n_0 , then p is determined up to an additive constant. If in addition $\rho(t)$ is known for some $t > 0$, then this additive constant is fixed, i.e., p is unique.*

Remark 4.5. *If the second component of a critical couple (\bar{t}, \bar{x}) is perturbed by noise $\delta \in \mathbb{R}$, and $n_0(\bar{x} + \delta) > 0$, then the reconstruction is given by*

$$p'(\bar{x} + \delta) = -\frac{n'_0(\bar{x} + \delta)}{\bar{t}n_0(\bar{x} + \delta)}.$$

Assuming smoothness of n_0 , a Taylor expansion yields the error estimate

$$p'(\bar{x}) - p'(\bar{x} + \delta) = O\left(\frac{\delta n'_0(\bar{x})^2 - n''_0(\bar{x})n_0(\bar{x})}{\bar{t}n_0(\bar{x})^2}\right) = O(\delta), \quad \text{as } \delta \rightarrow 0. \quad (4.5)$$

Hence, the corresponding inverse problem is stable. For a fixed $\delta > 0$, the error can, however, be large for $\bar{t}n_0(\bar{x})$ small, which can also be seen in the numerical examples below.

4.3 Remarks on simultaneous identification

Simultaneous identification of multiple parameters or their derivatives is difficult. Counting dimensions, it is to be expected that measurements of the one dimensional function $\rho(t)$ is not sufficient to simultaneously recover two parameter functions, which is supported by the following examples:

- (i) Let n_0 be any compactly supported function with $\int n_0 dx = a > 0$. Let $d_1(x)$ and $d_2(x)$ be arbitrary functions, and define $p_i(x) = ad_i(x)$, $i = 1, 2$. Then $n_i(x, t) = n_0(x)$ solves (1.1)–(1.2) with $\rho_i(t) = \rho(0) = a$. Hence, knowledge of ρ does not allow to identify p and d simultaneously.
- (ii) Let n_0 be any function supported on $[0, 1]$, $d = 0$, and let $p_i : [0, 1] \rightarrow [0, 1]$, $i = 1, 2$, be two invertible functions that satisfy $p_i(0) = 0$ and $p_i(1) = 1$. We define the initial datum as $n_0^i(x) = n_0(p_i(x))p'_i(x)$, and denote n_i the corresponding solutions to (1.1)–(1.2). Using the substitution $y = p_i(x)$, we obtain that

$$\rho_i(t) = \int_0^1 n_0^i(x) e^{p_i(x)t} dx = \int_0^1 n_0(y) e^{yt} dy,$$

i.e., $\rho_1(t) = \rho_2(t)$. Hence, it is not possible to determine n_0 and p from ρ . This argument can be extended to $d > 0$.

In Section 4.2, we have seen that measuring the critical couples of n allows for reconstruction of derivatives of one of the parameters. The discussion in Section 4.1 shows that if (\bar{t}_1, \bar{x}) and (\bar{t}_2, \bar{x}) are critical couples of n for $\bar{t}_1 \neq \bar{t}_2$, then $n'_0(\bar{x})$ and $p'(\bar{x})$ are uniquely determined with value 0 given that $d \in \mathbb{R}$ is constant. Similarly, $n'_0(\bar{x}) = 0$ and $d'(\bar{x}) = 0$ if $p \in \mathbb{R}$. Using (4.1), this reasoning can be extended to non-constant p and d , and to obtain formulas for $d'(\bar{x})$ and $p'(\bar{x})$ given $n'_0(\bar{x})/n_0(\bar{x})$ and $\rho(t)$, which is

$$\begin{pmatrix} \int_0^{\bar{t}_1} \rho(s) ds & -\bar{t}_1 \\ \int_0^{\bar{t}_2} \rho(s) ds & -\bar{t}_2 \end{pmatrix} \begin{pmatrix} d'(\bar{x}) \\ p'(\bar{x}) \end{pmatrix} = \frac{n'_0(\bar{x})}{n_0(\bar{x})} \begin{pmatrix} 1 \\ 1 \end{pmatrix}.$$

We note that, in general, the matrix in the above linear system might be singular, thereby allowing for multiple solutions or none. We note that identifying two of the parameter functions from knowledge of ρ and curves $(\bar{t}, \bar{x}(t))$ of critical couples remains an open problem.

5 Reconstructions

5.1 Reconstructions from the total population size

In this section we assume knowledge of the total population size $\{\rho(t) : 0 \leq t \leq T\}$ in order to determine the parameter function $p(x)$. Theorem 3.1 shows that measuring the total population size is sufficient in order to uniquely reconstruct the parameter p as long as d is a constant and p is either strictly increasing or strictly decreasing. Contrary to the situation of Theorem 4.2, there are, however, no explicit reconstruction formulas available. We thus propose to use a variational regularization technique to numerically reconstruct p from measurements of the (noisy) total population size $\rho^\delta(t)$, where $\delta > 0$ denotes the noise level. In the following two subsections we discuss two approaches to define suitable Tikhonov regularizations in Hilbert spaces.

5.1.1 Fully nonlinear forward operator

We begin with the obvious definition of the nonlinear forward operator

$$F : X = H^1(\mathcal{S}) \rightarrow Y = L^2(0, T), \quad p \mapsto \rho \quad \text{where} \quad \rho = \Lambda_p(\rho),$$

where Λ_p is defined in Lemma 2.2. The choice of $X = H^1(\mathcal{S})$ is motivated by the compactness of the embedding $H^1(\mathcal{S}) \hookrightarrow L^\infty(\mathcal{S})$, which implies that F is well-defined by Theorem 2.1 and that F is compact by Lemma 2.2. Here and in the following, \mathcal{S} denotes the interior of the support of n_0 . Denoting by $p_0 \in H^1(\mathcal{S})$ some a-priori knowledge, such as a monotonically increasing function, we construct stable approximations to the exact solution p^\dagger , which satisfies $F(p^\dagger) = \rho$, by minimizing the Tikhonov functional

$$J_\alpha^\delta(p) = \frac{1}{2} \|F(p) - \rho^\delta\|_Y^2 + \frac{\alpha}{2} \|p - p_0\|_X^2, \quad (5.1)$$

over the closed and convex set $\mathcal{D}(F) = \{p \in H^1(\mathcal{S}) : p' \geq \gamma > 0\}$ for some arbitrary but fixed constant $\gamma > 0$. The choice of $\mathcal{D}(F)$ is motivated by Theorem 3.1 where strictly monotone parameters p are considered. We make the assumption that the data perturbation can be estimated as follows

$$\|\rho - \rho^\delta\|_{L^2(0, T)} \leq \delta. \quad (5.2)$$

Standard theory of inverse problems can be used to prove existence of minimizers p_α^δ of J_α^δ and stable dependence on the data as long as $\alpha > 0$, see e.g. [9]. Widely used algorithms to minimize the Tikhonov functional employ the gradient of F . Without proof (which amounts to a lengthy calculation using (2.1)), we note that F depends smoothly on p and the Fréchet derivative is

$$F'(p) : h \mapsto D \quad \text{where} \quad D(t) = \int_{\mathbb{R}} \left[th(x) - d(x) \int_0^t D(s) ds \right] n_0(x) e^{pt-d \int_0^t \rho ds} dx,$$

for $p, h \in H^1(\mathcal{S})$. We observe that the definition of $F'(p)h$ constitutes an ordinary differential equation for $\int_0^t D(s) ds$, which yields the explicit formula

$$(F'(p)h)(t) = D(t) = \int_{\mathbb{R}} h(x) n_0(x) \int_0^t \left(\int_0^s e^{pr} dr \right) e^{-d \int_0^s \rho(r) dr} ds dx.$$

Using this formula, it is straightforward to obtain a formula for the adjoint operator $F'(p)^*\psi$, $\psi \in L^2(0, T)$, which is defined as the solution to

$$\begin{aligned} -\Delta w + w &= n_0(x) \int_0^T \psi(t) \int_0^t \left(\int_0^s e^{p(x)r} dr \right) e^{-d \int_0^s \rho dr} ds dt & \text{in } \mathcal{S}, \\ \partial_n w &= 0 & \text{on } \partial\mathcal{S}. \end{aligned}$$

It is easy to verify that for all $h, p \in H^1(\mathcal{S})$ and $\psi \in L^2(0, T)$

$$(F'(p)h, \psi)_{L^2(0, T)} = (h, F'(p)^*\psi)_{H^1(\mathcal{S})}.$$

Using the a-priori choice rule $\alpha \sim \delta$ and assuming the source condition

$$p^\dagger - p_0 = F'(p^\dagger)^*\xi \tag{5.3}$$

with sufficiently small $\xi \in L^2(0, T)$, $p_0 \in H^1(\mathcal{S})$ and that $p^\dagger \in \mathcal{D}(F)$, we obtain the convergence rates [9, Thm 10.4]

$$\|p_\alpha^\delta - p^\dagger\|_{H^1(\mathcal{S})} = O(\sqrt{\delta}), \quad \|\rho^\delta - F(p_\alpha^\delta)\|_{L^2(0, T)} = O(\delta). \tag{5.4}$$

In order to minimize the Tikhonov functional, we use the projected iteratively regularized Gauss-Newton (PIRGN) method

$$\begin{aligned} \tilde{p}_{k+1} &= p_k + (F'(p_k)^*F'(p_k) + \alpha_k I)^{-1} (F'(p_k)^*(\rho^\delta - F(p_k)) + \alpha_k(p_k - p_0)), \\ p_{k+1} &= \mathcal{P}_{\mathcal{D}(F)}(\tilde{p}_{k+1}) \end{aligned}$$

with $\alpha_k = \max\{\alpha, 1/2^k\}$. Here, $\mathcal{P}_{\mathcal{D}(F)}$ denotes the metric projection onto $\mathcal{D}(F)$ with respect to the $H^1(\mathcal{S})$ -norm; see [1] for a convergence analysis if $\alpha = 0$, $\delta \geq 0$, and the iteration is terminated after k^* steps with a-priori choice rule $\alpha_{k^*} \sim \delta$. The IRGN method combined with the discrepancy principle as a-posteriori stopping rule has been analyzed in [13] while an analysis of the PIRGN method can be found in [1, 12]. Let us refer to [8] for a discussion on the use of the PIRGN method to minimize (5.1) with $\alpha > 0$.

Numerical example We illustrate the performance of the PIRGN method choosing the example $n_0(x) = \cos(\pi x/2)$, for $x \in \mathcal{S} = (-1, 1)$, $p^\dagger(x) = e^x$, and $d(x) = 1$. The final time is chosen as $T = 1$. We choose a spatial grid with spacing 10^{-3} and temporal grid with spacing 10^{-2} . The initial guess p_0 is chosen such that it satisfies (5.3) with $\xi(t) = e^{-t}$, and the regularization parameter is chosen as $\alpha = \delta$. The data perturbation is computed via $\rho^\delta = \rho + \delta\eta$, where η is drawn from a normal distribution with mean 0 and variance 1, and then scaled such that $\|\eta\|_{L^2(0, T)} = 1$. The PIRGN iteration is stopped as soon as $\|\nabla J_\alpha^\delta(p_\alpha^\delta)\|_{H^1(\mathcal{S})} < 10^{-13}$. We observed that the iterates \tilde{p}_k all were positive and monotonically increasing, and the application of the metric projection was not necessary. A reconstruction is shown in Figure 1 together with the error $\|p_\alpha^\delta - p^\dagger\|_{H^1(\mathcal{S})}$, which exhibits the rate $O(\sqrt{\delta})$ as predicted by (5.4). The good convergence behavior of the PIRGN method can also be seen in Table 1.

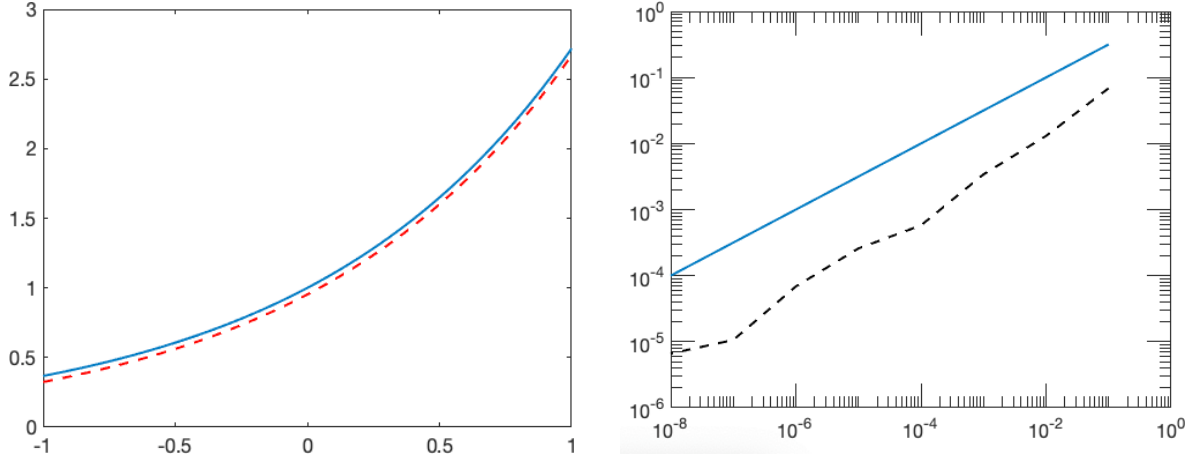


Figure 1: Left: p^\dagger (solid line) and corresponding reconstruction p_α^δ for $\alpha = \delta = 0.1$ (dotted curve). Right: A plot of the error $\|p_\alpha^\delta - p^\dagger\|_{H^1(S)}$ (dotted) and the curve $\sqrt{\delta}$ (solid) for different values of δ .

Table 1: Convergence behavior of the PIRGN method for the minimization of (5.1) for different noise levels δ together with the iteration count k of the PIRGN method. The error converges with $O(\sqrt{\delta})$, cf. Figure 1.

δ	$\ p_\alpha^\delta - p^\dagger\ _{H^1(S)}$	$\ \rho^\delta - F(p_\alpha^\delta)\ _{L^2(0,T)}$	k
10^{-1}	6.9×10^{-2}	1.07δ	10
10^{-2}	1.3×10^{-2}	1.13δ	12
10^{-3}	3.4×10^{-3}	1.15δ	14
10^{-4}	5.8×10^{-4}	1.17δ	17
10^{-5}	2.6×10^{-4}	1.17δ	19
10^{-6}	6.9×10^{-5}	1.17δ	22
10^{-7}	1.1×10^{-5}	1.17δ	25
10^{-8}	6.6×10^{-6}	1.17δ	28

5.1.2 Perturbed forward operator

In order to reduce the nonlinearity of the inverse problem, let us present a second choice of forward operator. Using the data ρ^δ in the right hand side of (2.2), we define a perturbed forward operator

$$F^\delta(p) = \Lambda_p(\rho^\delta) = \int_{\mathbb{R}} n_0(x) e^{tp(x)-d(x)} \int_0^t \rho^\delta(s) ds dx,$$

which is well-defined for $p \in H^1(\mathcal{S})$. Using Lemma 2.2, we have that F^δ depends continuously on ρ^δ in the $L^2(0, T)$ -topology and on p in the $L^\infty(\mathcal{S})$ -topology. Since the embedding $H^1(\mathcal{S}) \hookrightarrow L^\infty(\mathcal{S})$ is compact, we deduce that $F^\delta : H^1(\mathcal{S}) \rightarrow L^2(0, T)$ is a compact operator. Writing $F^0(p) = \Lambda_p(\rho)$, we have that $F^0(p^\dagger) = F(p^\dagger)$ and

$$\|F^\delta(p^\dagger) - F(p^\dagger)\|_{L^2(0, T)} \leq \|n_0\|_{L^1} e^{T\|p^\dagger\|_\infty} \|d\|_\infty T \|\rho^\delta - \rho\|_{L^2(0, T)}. \quad (5.5)$$

Thus, in view of standard results from the analysis of Tikhonov regularization [9], we can obtain stable approximations by minimizing the following Tikhonov functional with perturbed forward operator

$$\tilde{J}_\alpha^\delta(p) = \frac{1}{2} \|F^\delta(p) - \rho^\delta\|_Y^2 + \frac{\alpha}{2} \|p - p_0\|_X^2 \quad (5.6)$$

over $\mathcal{D}(F^\delta) = \mathcal{D}(F)$ to enforce strict monotonicity of the minimizers. Convergence of the minimizers for $\delta \rightarrow 0$ is established in the next lemma, which is an adaptation of [9, Thm. 10.3].

Lemma 5.1. Let $\alpha = \alpha(\delta)$ be such that $\alpha(\delta) \rightarrow 0$ and $\delta^2/\alpha(\delta) \rightarrow 0$ as $\delta \rightarrow 0$. Denote by $\{p_\alpha^\delta\} \subset \mathcal{D}(F^\delta)$ a sequence of minimizers of (5.6), where the data ρ^δ satisfies (5.2). Then

$$\lim_{\delta \rightarrow 0} p_{\alpha(\delta)}^\delta = p^\dagger \quad \text{in } H^1(\mathcal{S}).$$

Proof. The proof is similar to [9, Thm. 10.3]. Since $\{p_\alpha^\delta\}$ minimize (5.6), we have that

$$\begin{aligned} \frac{1}{2} \|F^\delta(p_\alpha^\delta) - \rho^\delta\|_Y^2 + \frac{\alpha}{2} \|p_\alpha^\delta - p_0\|_X^2 &\leq \frac{1}{2} \|F^\delta(p^\dagger) - \rho^\delta\|_{L^2(0, T)}^2 + \frac{\alpha}{2} \|p^\dagger - p_0\|_X^2 \\ &\leq 2C(\|p^\dagger\|_X)^2 \delta^2 + \frac{\alpha}{2} \|p^\dagger - p_0\|_X^2, \end{aligned}$$

where we used (5.5) in the last step. Hence, $\limsup_{\delta \rightarrow 0} \|p_\alpha^\delta - p_0\|_X^2 \leq \|p^\dagger - p_0\|_X^2$ and $\{p_\alpha^\delta\}$ is bounded in $H^1(\mathcal{S})$ and has a weakly convergent subsequence $\{p_{\alpha_k}^{\delta_k}\}$ with limit $p \in \mathcal{D}(F^\delta)$. Due to the compactness of the embedding $H^1(\mathcal{S}) \hookrightarrow L^\infty(\mathcal{S})$, this subsequence also converges strongly to p in $L^\infty(\mathcal{S})$. Moreover, we have that

$$\|F^\delta(p_\alpha^\delta) - \rho^\delta\|_Y^2 \leq 4C(\|p^\dagger\|_X)^2 \delta^2 + \alpha \|p^\dagger - p_0\|_X^2.$$

By taking the limit $\delta \rightarrow 0$ and using continuity of F^δ with respect to p in $L^\infty(\mathcal{S})$ and ρ^δ in Y , we deduce that $F^0(p) = \rho$, i.e., ρ is a fixed point of Λ_p , and, thus $F(p) = F(p^\dagger)$. The uniqueness result of Theorem 3.1 then implies $p = p^\dagger$. A subsequence argument implies weak convergence of the whole sequence $\{p_\alpha^\delta\}$ to p^\dagger in $H^1(\mathcal{S})$. Since

$$\limsup_{\delta \rightarrow 0} \|p_\alpha^\delta - p^\dagger\|_X^2 = \limsup_{\delta \rightarrow 0} (\|p_\alpha^\delta - p_0\|_X^2 + \|p^\dagger - p_0\|_X^2 - 2\langle p_\alpha^\delta - p_0, p^\dagger - p_0 \rangle) \leq 0,$$

we obtain norm convergence of p_α^δ to p^\dagger . \square

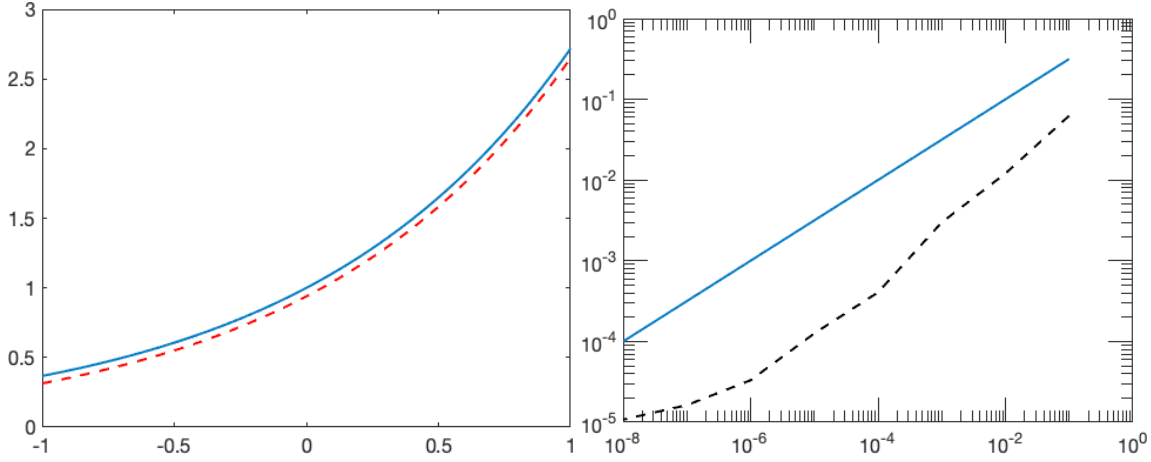


Figure 2: Left: p^\dagger (solid line) and corresponding minimizer p_α^δ of (5.6) for $\alpha = \delta = 0.1$ (dotted line). Right: A plot of the corresponding errors $\|p_\alpha^\delta - p^\dagger\|_{H^1(S)}$ (dotted) and the curve $\sqrt{\delta}$ (solid) for different values of δ .

The perturbed forward operator F^δ is Fréchet differentiable with derivative

$$dF^\delta(p)h = \int_{\mathcal{S}} h(x)n_0(x)te^{pt-d\int_0^t \rho^\delta ds} dx, \quad h \in H^1(\mathcal{S}),$$

and the adjoint $dF^\delta(p)^*\psi$, $\psi \in L^2(0, T)$, is defined as the solution to

$$\begin{aligned} -\Delta w + w &= n_0(x) \int_0^T t\psi(t)e^{pt-d\int_0^t \rho^\delta ds} dt & \text{in } \mathcal{S}, \\ \partial_n w &= 0 & \text{on } \partial\mathcal{S}. \end{aligned}$$

The Tikhonov functional (5.6) can then be minimized as above by the PIRGN method, which we consider next.

Numerical Example We consider the same example and setup as in the previous section. In particular, we use the source condition (5.3) for the unperturbed forward operator. We observe, that using the perturbed forward operator yields essentially the same results as using the fully nonlinear forward operator. However, the numerical implementation of the perturbed forward operator is simpler. Figure 2 shows an exemplary reconstruction together with the exact solution and the convergence behaviour of the error $\|p_\alpha^\delta - p^\dagger\|_{H^1(S)}$ for different values of δ . Table 2 shows, in addition, the convergence of the residuals for different values of δ and the required PIRGN iterations to obtain a suitable reconstruction. A theoretical explanation of the observed convergence rates for the error remains open.

5.2 Reconstructions using critical points of the population density

We illustrate the reconstruction formulas given in Theorem 4.2 by numerical examples. Contrary to Theorem 3.1, Theorem 4.2 does not require monotonicity of the parameter functions.

Table 2: Convergence behavior of the PIRGN method for the minimization of (5.6) for different noise levels δ together with the iteration count k of the PIRGN method. The error converges with $O(\sqrt{\delta})$, cf. Figure 2.

δ	$\ p_\alpha^\delta - p^\dagger\ _{H^1(\mathcal{S})}$	$\ \rho^\delta - F^\delta(p_\alpha^\delta)\ _{L^2(0,T)}$	k
10^{-1}	6.3×10^{-2}	1.03δ	11
10^{-2}	1.2×10^{-2}	1.04δ	13
10^{-3}	3.0×10^{-3}	1.04δ	14
10^{-4}	4.1×10^{-4}	1.05δ	17
10^{-5}	1.3×10^{-4}	1.04δ	19
10^{-6}	3.3×10^{-5}	1.04δ	22
10^{-7}	1.6×10^{-5}	1.04δ	25
10^{-8}	1.1×10^{-5}	1.02δ	29

Reconstruction of p' from critical points of n As an initial datum we choose $n_0(x) = \cos(\pi x/2)$, $d(x) = 1$ and $p(x) = 1 + \sin(x)^2$ and we let $x \in (-1, 1)$ and $t \in [0, 10]$. For our numerical computations, we discretize x equidistantly with grid spacing 10^{-4} . Similarly, we discretize time with time step size 10^{-2} . In our numerical algorithms, given an approximation of $n(t, x)$ we thus compute $\rho(t)$ and $\int_0^t \rho(s) ds$ approximately using quadrature rules. Using these approximations, we compute an approximation of n at the next time instance using (2.1) with $\int_0^t \rho(s) ds$ replaced by its numerical approximation.

To apply Theorem 4.2, we collect the minima and maxima of the approximate population density over time as our data $\{(\bar{t}_i, \bar{x}_i)\}$; cf. Figure 3 for snapshots of the approximation of $n(t, x)$ for $t \in \{2, 6, 9\}$. Since $n'_0(x)p'(x) \leq 0$ for all $x \in (-1, 1)$, all $x \in (-1, 1)$ will eventually induce a critical couple: $(\bar{t}, 0)$ is a critical couple for all $\bar{t} \geq 0$, while (\bar{t}, \bar{x}) with $\bar{x} \neq 0$ is a critical couple of n for exactly one $\bar{t} > 0$, see Section 4.1. In Figure 4 the corresponding reconstruction p'_r of p' is shown. As predicted by Theorem 4.2, we observe excellent agreement of the reconstruction with p' , which is to be expected for highly resolved numerical approximations.

If we add 2.5% of uniformly distributed noise to the location of the critical points, i.e., the data is changed to $\{(t_i, \bar{x}_i(1 + \delta\eta_i))\}$ with $\eta_i \sim U(-1/2, 1/2)$ and $\delta = 0.05$, the reconstructions deteriorate slightly for small values of $t_i n_0(\bar{x}_i)$ as quantified in Remark 4.5, see Figure 4. As argued in Remark 4.5 and shown in Figure 4, for sufficiently small noise, we obtain a linear rate of convergence in δ of the reconstruction error

$$\sup_i |p'(\bar{x}_i) - p'_r(\bar{x}_i(1 + \delta\eta_i))|,$$

showing well-posedness of the reconstruction problem if the initial data and its derivative are available. The saturation for small noise is due to the errors in the numerical approximation, and it can be overcome by using a finer discretization to generate the simulated data.

Reconstruction of d' from critical points of n The setting is similar to the previous example. The difference is that we choose $p(x) = 1$, $d(x) = 1 - x^2$, and simulate until $T = 3$. A similar discussion as for the previous example applies. In particular, since $d'(x)n'_0(x) > 0$, all $x \in (-1, 1)$ will eventually induce critical couples, see Section 4.1. Recording the critical couples of n and the total population allows for the reconstruction of the derivative of the

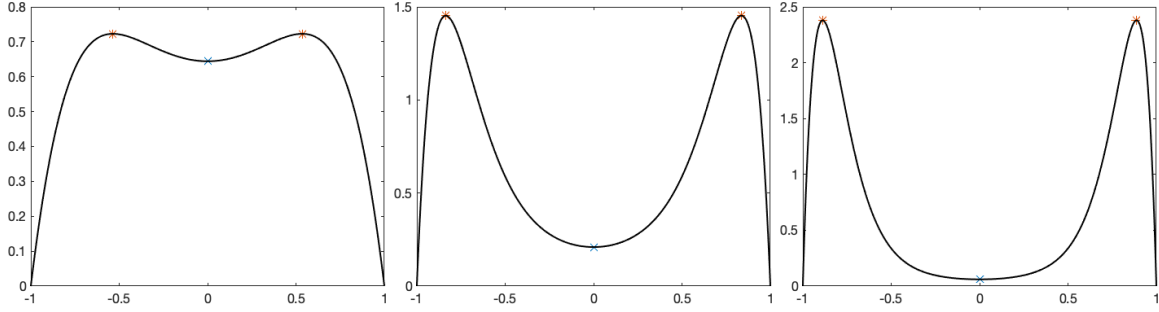


Figure 3: Snapshots of the numerical approximation of $n(t, x)$ for $t \in \{2, 6, 9\}$ for the reconstruction of p' (from left to right). The markers denote the corresponding critical points that are used in the reconstruction formula.

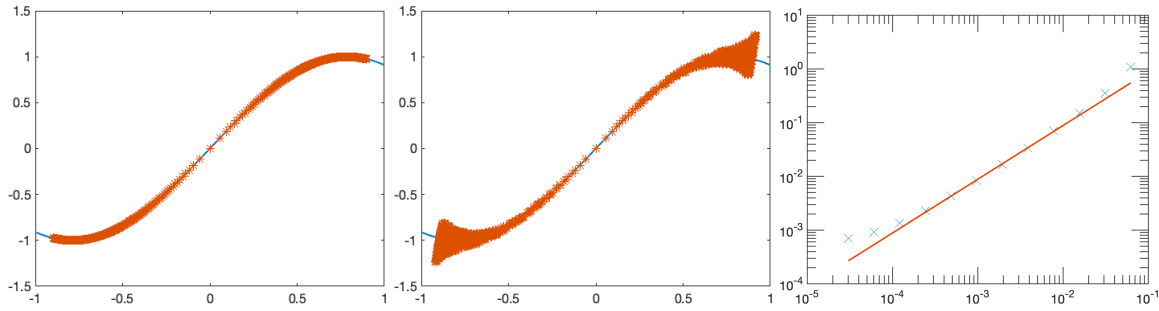


Figure 4: Numerical reconstructions of p' (red crosses) and the exact (unknown) function p' (solid blue line) are shown. Left for critical points that are located within the accuracy of the numerical scheme; middle critical points with 2.5% of uniform random noise. Right: Convergence rates for different noise levels $\delta = 1/2^i$ for $i = 4, \dots, 15$ (crosses), the solid curve is proportional to δ .

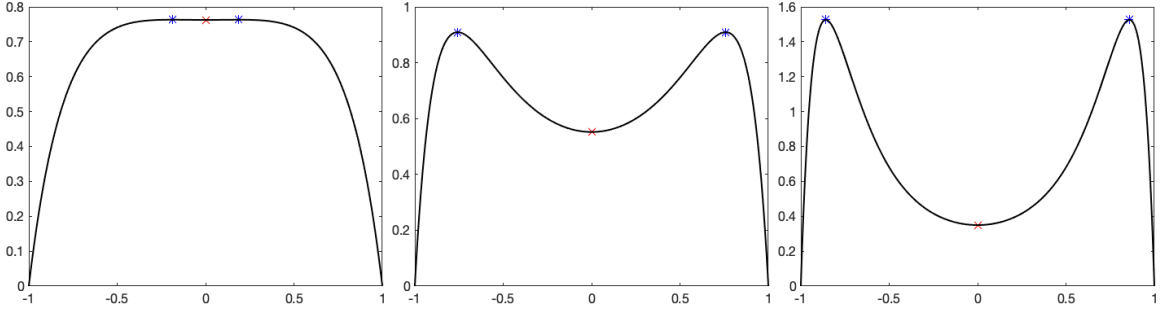


Figure 5: Snapshots of the numerical approximation of $n(t, x)$ for $t \in \{1, 2, 3\}$ for the reconstruction of d' (from left to right). The markers denote the corresponding critical points that are used in the reconstruction formula.

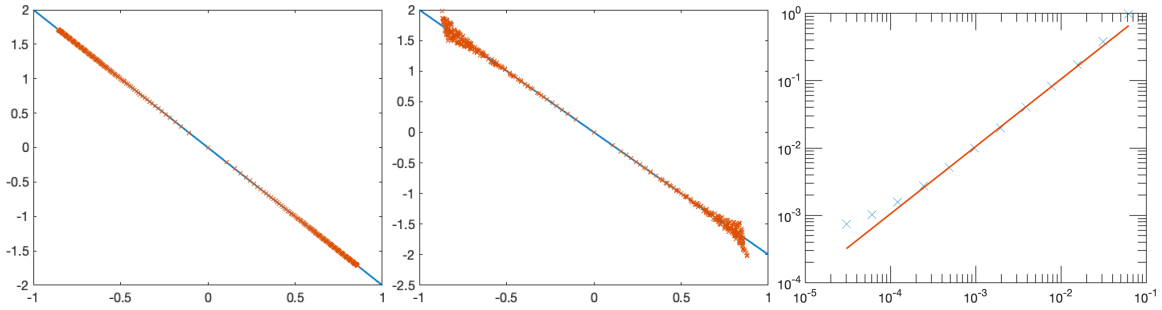


Figure 6: Numerical reconstructions of d' (red crosses) and the exact (unknown) function d' (solid blue line) are shown. Left for critical points that are located within the accuracy of the numerical scheme; middle critical points with 2.5% of uniform random noise. Right: Convergence rates for different noise levels $\delta = 1/2^i$ for $i = 4, \dots, 15$ (crosses), the solid curve is proportional to δ .

unknown parameter d if the initial datum is given. Adding relative noise to the critical points will deteriorate the reconstruction only slightly; again showing well-posedness of the reconstruction problem.

6 Conclusions and outlook

We considered several inverse problems for a nonlinear structured population model, whose dynamics is governed by a nonlocal averaging process. More precisely, we investigated the reconstruction of model parameters given either the total population size or the critical points of the population density. We demonstrated that in both cases the model possesses several symmetries that leave the measurements invariant, showing the limited information content of the total population size or the critical couples as the only measurements. Ruling out these situations by appropriate assumptions on the unknown quantities, we obtained uniqueness results and in some cases explicit reconstruction formulas.

In order to model local interactions due to (small) mutations, the following generalization in

the form of a parabolic system has been derived in [4]:

$$\begin{aligned}\partial_t n(t, x) - \Delta n(t, x) &= \left[p(x) - \int_{\mathbb{R}} d(x, y) n(t, y) dy \right] n(t, x), \\ n(0, x) &= n_0(x),\end{aligned}$$

where $d(x, y)$ allows to model more general competition behaviour. In this case, we are dealing with a second order parabolic equation and the explicit formula (2.1) is no longer available, which requires the use of different methods. We expect that some of our results can be extended to this case as well, e.g., by using the heat kernel to obtain a fixed point equation for ρ . In particular, in such a setup using a perturbed forward operator as in Section 5.1.2 will yield a significant speed up in numerical computations. The investigation of such a model is, however, out of the scope of this paper and is left for future study.

Acknowledgements

JFP acknowledges support by the German Science Foundation DFG via EXC 1003 Cells in Motion Cluster of Excellence, Münster. The authors would like to thank Barbara Kaltenbacher (Klagenfurt) for stimulating discussions.

References

- [1] A. B. Bakushinsky and M. Y. Kokurin. *Iterative Methods for Approximate Solution of Inverse Problems*, volume 577 of *Mathematics and its Applications*. Springer, Dordrecht, 2004.
- [2] G. Barabás and G. Meszéna. When the exception becomes the rule: The disappearance of limiting similarity in the Lotka–Volterra model. *Journal of Theoretical Biology*, 258(1):89 – 94, 2009.
- [3] Pablo Chamoso, William Raveane, Victor Parra, and María Angélica González Arrieta. Uavs applied to the counting and monitoring of animals. In *ISAmI*, 2014.
- [4] N. Champagnat, R. Ferrière, and S. Méléard. Unifying evolutionary dynamics: From individual stochastic processes to macroscopic models. *Theoretical Population Biology*, 69(3):297 – 321, 2006. ESS Theory Now.
- [5] N. Champagnat, R. Ferrière, and S. Méléard. From individual stochastic processes to macroscopic models in adaptive evolution. *Stochastic Models*, 24(sup1):2–44, 2008.
- [6] L. Desvillettes, P.-E. Jabin, S. Mischler, and G. Raoul. On selection dynamics for continuous structured populations. *Commun. Math. Sci.*, 6(3):729–747, 09 2008.
- [7] U. Dieckmann and R. Law. The dynamical theory of coevolution: a derivation from stochastic ecological processes. *Journal of Mathematical Biology*, 34(5):579–612, May 1996.
- [8] H. Egger and M. Schlottbom. Numerical methods for parameter identification in stationary radiative transfer. *Comput. Optim. Appl.*, 62(1):67–83, 2015.

- [9] H. W. Engl, M. Hanke, and A. Neubauer. *Regularization of inverse problems*, volume 375 of *Mathematics and its Applications*. Kluwer Academic Publishers Group, Dordrecht, 1996.
- [10] S. Fodelianakis, A. Lorz, A. Valenzuela-Cuevas, A. Barozzi, J. M. Booth, and D. Dafonchio. Dispersal homogenizes communities via immigration even at low rates in a simplified synthetic bacterial metacommunity. *Nature Communications*, 10, 2019.
- [11] P.-E. Jabin and G. Raoul. On selection dynamics for competitive interactions. *J. Math. Biol.*, 63(3):493–517, 2011.
- [12] B. Kaltenbacher and A. Neubauer. Convergence of the projected iterative regularization methods for nonlinear problems with smooth solutions. *Inverse Problems*, 22:1105–1119, 2006.
- [13] B. Kaltenbacher, A. Neubauer, and O. Scherzer. *Iterative Regularization Methods for Nonlinear Ill-Posed Problems*, volume 6 of *Radon Series on Computational and Applied Mathematics*. de Gruyter, Berlin, New York, 2008.
- [14] A. Lorz, T. Lorenzi, J. Clairambault, A. Escargueil, and B. Perthame. Modeling the effects of space structure and combination therapies on phenotypic heterogeneity and drug resistance in solid tumors. *Bulletin of Mathematical Biology*, 77(1):1–22, 2015.
- [15] A. Lorz, S. Mirrahimi, and B. Perthame. Dirac mass dynamics in multidimensional non-local parabolic equations. *Communications in Partial Differential Equations*, 36(6):1071–1098, 2011.
- [16] A. Lorz and B. Perthame. Long-term behaviour of phenotypically structured models. *Proc. R. Soc. Lond. Ser. A Math. Phys. Eng. Sci.*, 470(2167):20140089, 10, 2014.
- [17] J. Maynard Smith and G. R. Price. The logic of animal conflict. *Nature*, 246:15–18, 1973.
- [18] J. Roughgarden. *Theory of Population Genetics and Evolutionary Ecology: An Introduction*. Macmillan, 1979.
- [19] S. Sieuwerts, F.A.M. De Bok, E. Mols, W.M. De Vos, and J.E.T. Van Hylckama Vlieg. A simple and fast method for determining colony forming units. *Letters in Applied Microbiology*, 47(4):275–278, 2008.